Structure, Vol. 12, 1057–1065, June, 2004, ©2004 Elsevier Ltd. All rights reserved. DOI 10.1016/j.str.2004.03.022

RIα Subunit of PKA: A cAMP-free Structure Reveals a Hydrophobic Capping Mechanism for Docking cAMP into Site B

Jian Wu,[1] Simon Brown,[2] Nguyen-Huu Xuong,[1,3] and Susan S. Taylor[1,2,*]
[1]Department of Chemistry and Biochemistry
[2]Howard Hughes Medical Institute
[3]Department of Biology and Physics
University of California, San Diego
La Jolla, California 92093

Summary

In eukaryotes the primary target for cAMP, a ubiquitous second messenger, is cAMP-dependent protein kinase (PKA). Understanding how binding and release of cAMP changes the cAMP binding domains and then triggers long-range allosteric responses is an important challenge. This conformational switching requires structure solutions of cAMP binding domains in cAMP-bound and cAMP-free states. We describe for the first time a crystal structure of the cAMP binding domains of PKA type Iα regulatory subunit where site A is occupied by cGMP and site B is unoccupied. The structure reveals that the carboxyl terminus of domain B serves as a hydrophobic cap, locking the cyclic nucleotide via its adenine ring into the β-barrel. In the absence of cAMP, the "cap" is released via an extension of the C-terminal helix. This simple hinge mechanism for binding and release of cAMP also provides a mechanism for allosteric communication between sites A and B.

Introduction

Cyclic AMP (cAMP) is an ancient signaling molecule that triggers an intracellular biological response initiated by an extracellular signal. The module to which cAMP binds is also a highly conserved domain that is found in all cells. In bacteria this cAMP binding module is frequently linked to a transcription factor (CAP) (Mitra et al., 1975), whereas in mammals it is linked to protein kinase activation (PKA, PKG) (Walsh et al., 1968; Taylor et al., 1990), to cyclic nucleotide-gated channels (Ludwig et al., 1990), and to guanine nucleotide exchange factors (EPAC) (de Rooij et al., 1998; Kawasaki et al., 1992). Scanning of genomes reveals that there are many other modules that are fused to this cyclic nucleotide binding module (Shabb and Corbin, 1992). The ligand and its binding domain thus constitute a ubiquitous signaling partnership that universally translates an external stimuli into a biological response. Frequently this signaling pathway is linked to nutrient deprivation. How the allosteric binding and release of cAMP leads to a change in the protein binding properties of this module constitutes one of the most ancient allosteric processes in biology.

The cAMP binding module is comprised of two subdomains, a contiguous eight-stranded β-barrel that serves as the docking site for the cyclic nucleotide and a noncontiguous helical subdomain that serves as a docking site for interacting with other proteins or domains (Huang and Taylor, 1998). The mechanism by which the binding of cAMP allosterically regulates this helical domain as it toggles between two different conformational states is still not well resolved. The crystal structures of eight cAMP binding domains are now known: four cAMP binding domains have been crystallized in the RIα and RIIβ regulatory subunits (R) of PKA (Su et al., 1995; Diller et al., 2001), the cAMP binding domain of CAP which is fused to a DNA binding domain (Weber and Steitz, 1987), the two cAMP binding domains of EPAC (Rehmann et al., 2003), and the recently solved cAMP-gated channel (Zagotta et al., 2003). The first five structures have been crystallized only in the presence of cAMP, whereas EPAC has been crystallized only in the absence of cAMP. The cAMP-gated channel was crystallized in the presence of cAMP and cGMP, respectively. To fully understand the conformational constraints that are imposed by the binding of cAMP, it is essential not only to have a structure of the cAMP bound state but also of a cAMP-free state. In addition, solution methods are essential for understanding the dynamics of this conformational switch. Using hydrogen/ deuterium exchange, coupled with mass spectrometry, we have shown that the conformational change in the cAMP binding domains of the RIα and RIIβ subunits of PKA when cAMP is removed is small but long range (Anand et al., 2002), and this is confirmed by molecular dynamic calculations of RIα (D. Vigil and S.S.T., unpublished data). A comparison of RIα and RIIβ with CAP, as well as the crystal structure of the unliganded form of the EPAC cAMP binding domains, suggest a hinge mechanism for the coupling of the helical and β-barrel subdomains.

The regulatory subunits of PKA are typically dimeric proteins that are joined at the amino terminus by a small stable helical domain that serves also as a docking site for A kinase anchoring proteins (APAPs) (Rubin, 1994; Banky et al., 2003). The two tandem cAMP binding domains lie at the C terminus. The isoform-specific linker region, in the absence of the catalytic subunit (C), is quite disordered and becomes partially ordered upon binding of C (Su et al., 1995). The linker region contains either a pseudosubstrate site (RIα and RIβ) or a substrate site (RIIα and RIIβ) (Scott, 1991) that docks to the active site cleft of the C subunit thereby rendering the enzyme inactive. A secondary site of interaction, localized in RIα to cAMP binding domain A, conveys high-affinity (0.2 nM) binding of the R subunit (Huang and Taylor, 1998). In RIα the two cAMP binding sites play different roles. Site A is essential for binding to C and toggles between a cAMP-bound form and a C-bound form. Site B is thought to serve as a gatekeeper for site A; the prediction is that cAMP binds first to site B in the holoenzyme complex, and only when site B is occupied can cAMP bind to site A (Ogreid and Doskeland, 1981a, 1981b). The two sites also have different affinities for cAMP. Site B has a slow dissociation rate while cAMP

*Correspondence: staylor@ucsd.edu

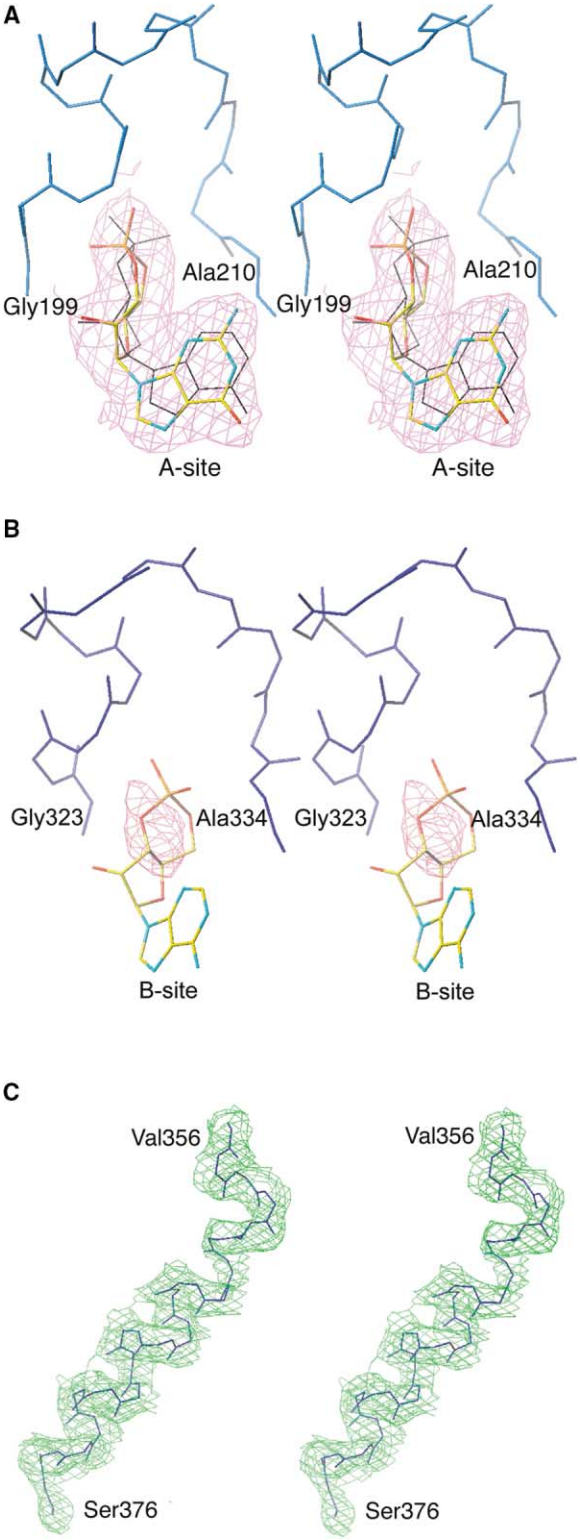

Figure 1. Stereoview of Density Maps

(A and B) The omit (Fo-Fc) maps of A site and B site, respectively, contoured at 3σ. The backbone traces of the PBC motifs are also shown. A cyclic GMP is modeled into (A). A cAMP, in black, is superimposed according to its position in the cAMP-bound structure. A cAMP, based on the structure of the cAMP-bound state, is built into (B) for tracking purpose only.

(C) The 2(Fo-Fc) map of the C-terminal tail, contoured at 1σ. Val356 and Ser376 are indicated.

exchanges more rapidly to site A (Rannels and Corbin, 1981; Døskeland et al., 1983). In solution, the cAMP binding sites remain saturated with cAMP even after prolonged dialysis.

By purifying the Δ(1-91) RIα subunit by cAMP affinity chromatography, and then eluting with cGMP and dialyzing, we isolated and then crystallized the cAMP-free protein. Here we show for the first time a crystal structure of the cAMP binding domains of RIα where site A is occupied by cGMP and site B is unoccupied. The structure reveals a hydrophobic cap at the carboxyl terminus of the RIα subunit, and this cap serves to lock the cyclic nucleotide via its adenine ring into the β-barrel. The structure provides a simple but elegant model for docking of the cyclic nucleotide and also provides a mechanism for interdomain communication between site A and site B mediated in part by the C helix.

Results

Overall Structure

In the absence of cyclic AMP, the Δ(1-91) deletion mutant of RIα crystallized in a $P6_5$ space group with two molecules in an asymmetric unit. The crystallization conditions were similar to those used to crystallize the cAMP-bound Δ(1-91) RIα, but the pH was 7.5 instead of 5.5. Δ(1-91) RIα with cAMP bound crystallized in $P6_522$ space group with one molecule in the asymmetric unit (Su et al., 1995). However, the crystal packing pattern overall is the same in the absence or presence of cAMP with the exemption of the carboxyl terminus.

The final model of Δ(1-91) RIα in its cAMP-free state contains two regulatory subunits, apoA and apoB, in the asymmetric unit, with continuous electron density throughout residues 109–376 in the apoA molecule and residues 109–367 in apoB. In both molecules, site A is occupied by a cyclic nucleotide, whereas site B is unoccupied. Figures 1A and 1B show the Fo-Fc omit maps in site A and site B, respectively. The well-defined electron density in site A can be attributed to cyclic GMP due to the cGMP elution method we used, even though cAMP and cGMP cannot unambiguously distinguished by X-ray at this low resolution (2.7 Å). To account for the small positive Fo-Fc density in site B, several water atoms and one glycerol molecule were built into site B, respectively. The glycerol molecule best fits the shape of the density.

The R factor and R_{free} are 24.0% and 28.5%, respectively (Table 1). The high values are likely due to the disorder of the first 16 residues at the N terminus, and the inherent flexibility of domain B due to the loss of ligand binding. The Ramachandran plot shows that the geometry of the model is good; 80.8% of all the nonglycine residues are located in the most favored regions, with the rest falling into the allowed regions. The rms deviation (rmsd) between apoA and apoB is 1.4 Å overall for all residues; for domain A it is only 0.41 Å, which implies that the domain B in the two molecules adopts an apparently more flexible conformation. When the A domains from apoA and apoB were superimposed, domain B is rotated slightly further away from the domain A in apoA compared to apoB, as shown in Figure 2A. The

Table 1. Crystal Data and Refinement Statistics

Space group	$P6_5$
Cell dimensions	
a = b (Å)	90.3
c (Å)	177.6
No. of molecules per asymmetric unit	2
Resolution range (Å)	50.0–2.7
R_{sym}[a]	0.053 (0.458)[b]
I/σ	14.1 (2.5)[b]
Data completeness (%)	93.6 (93.1)[b]
R factor (R_{free})	0.240 (0.285)
Rms deviation from ideality	
Bond lengths (Å)	0.009
Bond angles (°)	1.70

[a] R_{sym} = SUM (ABS (I − <I>))/SUM (I).
[b] The numbers in the parentheses correspond to the highest resolution shell.

higher overall average temperature factors (B factors) of domain B relative to domain A also suggests that removal of cAMP introduces enhanced dynamics into domain B (Figure 2B).

The RIα subunit in the cAMP-free state shows a similar conformation to previously solved ligand-bound structures overall: cAMP-bound state (PBD code of 1RGS), Rp-cAMP, and Sp-cAMP analog-bound states with PDB code of 1NE4 and 1NE6, respectively (Wu et al., 2004). Excluding the C-terminal tail, the overall rms deviation of apoA and 1RGS is 0.94 Å and that of apoB with 1RGS is 0.99 Å.

The most significant conformational changes in the RIα subunit between the cAMP-free state and cAMP-bound state appears at the carboxyl terminus, as shown as Figure 3. In the presence of cAMP, this segment, comprised of residues 357–376, folds around the B site binding pocket to seal the ligand like a "cap" into the phosphate binding pocket. Several contacts, representing both hydrophobic and hydrogen bonding, are associated with this C-terminal capping process. Tyr371 is one of the key residues that contributes to capping the B site cyclic AMP into the β-barrel core of domain B. This residue makes hydrophobic interactions by stacking its side chain phenol ring against the adenine ring of cAMP. Its hydroxyl group also contributes by hydrogen bonding

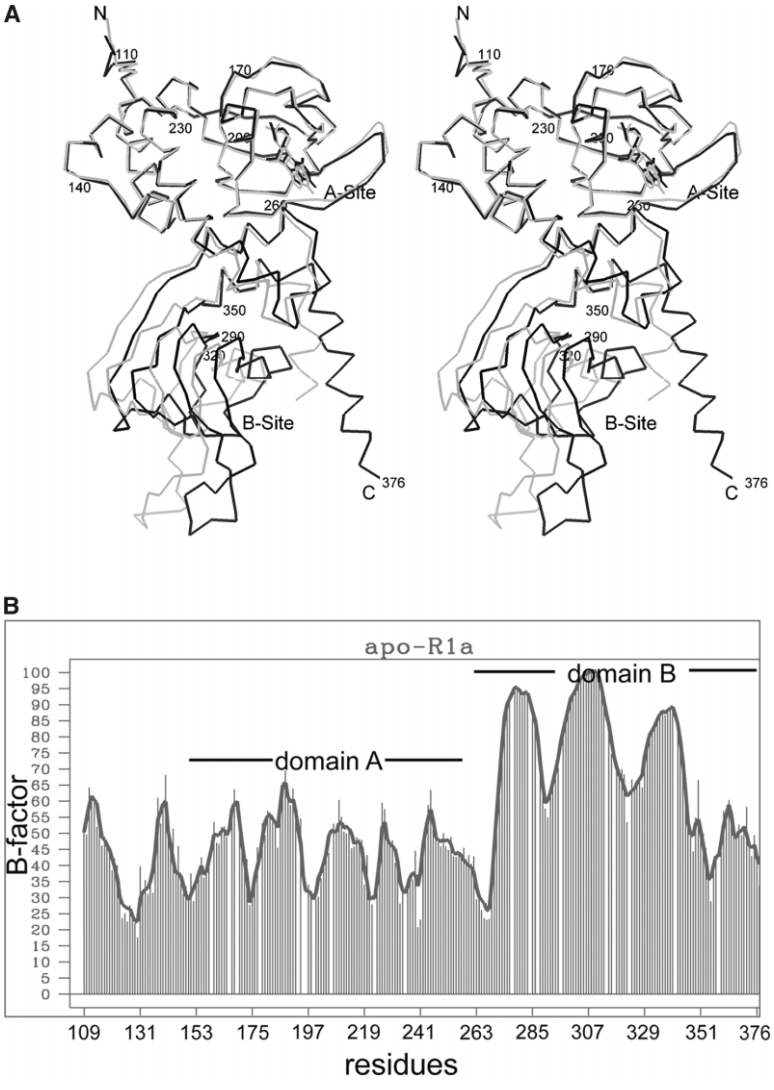

Figure 2. Dynamics of Domain B in the Absence of cAMP

(A) Superimposition of the two molecules (ApoA and ApoB) in the asymmetric unit. The two molecules are superimposed by their A domains to show that they differ in the overall orientation of domain B relative to domain A. ApoA is shown in black, and ApoB in gray. The N- and C termini are labeled. Residue numbers are added periodically to help track the Cα trace.

(B) The B factor plot of ApoA shows that the average B factors in domain B are significantly higher compared to domain A when the cyclic nucleotide was removed.

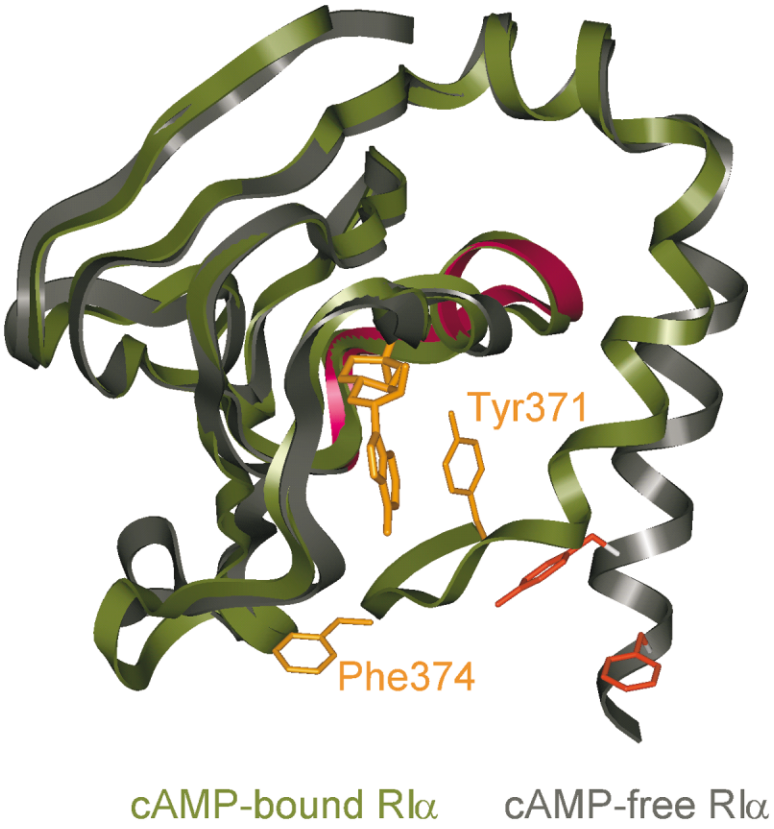

Figure 3. Ribbon Diagram of Domain B

Ribbon diagram of domain B in cAMP-free RIα (gray), superimposed with that of cAMP-bound RIα (tan). The C-terminal segment shows a clear hinge movement. Cyclic AMP in cAMP-bound RIα is shown. Tyr371 and Phe374 in both structures are shown.

to Glu324, an invariant residue in the phosphate binding cassette (PBC) of domain B. Glutamic acid 324, which is equivalent to Glu200 in the PBC of domain A, interacts with the hydroxyl moiety of the cAMP ribose ring and is also linked to the rest of the protein by an extensive network of contacts that are dependent on the presence of cAMP. Tyr371 is photoaffinity labeled almost stoichiometricaly by 8-N_3-cAMP bound to site B (Ringheim et al., 1988). Furthermore, mutagenesis of Tyr371 to Phe or Ala causes the K_d (cAMP) to increase from 16 to 60 nM, and the positive cooperativity between two cAMP binding sites is abolished (Bubis et al., 1988). These findings suggest that Tyr371 makes significant contributions to cAMP binding and stabilization of the domain through this hydrogen-bonding network.

In addition to Tyr371, the high-affinity binding of cAMP involves other interactions with the carboxyl terminus. In the site B cAMP binding pocket, the adenine ring of cAMP is sandwiched by hydrophobic interactions between the side chains of Val300, Val313, and Ala335 on one side and Leu316, Ile325, Tyr371, and Ser373 on the other. There is a weak hydrogen bond directly between the N6 atom of cAMP and the carbonyl oxygen of Asn372. Several other residues (Ser373, Phe374, and Val375) are also involved in an extensive hydrogen-bonding network with Gln302 from the β strand 4 in domain B. The latter residue is not conserved throughout the protein kinase family. The multiple contacts between the C-terminal tail, cAMP, and the B site pocket are summarized in Tables 2 and 3 and Figure 3.

In the absence of cAMP, the C-terminal tail moves away from the cAMP binding pocket, causing the "gate" to open (Figure 3). This release of the cap extends the C helix. An apparent allosteric movement can be traced

Table 2. Hydrogen Bonds Involving the C-Terminal Tail when cAMP Bounded

Atom 1 (from C tail)	Atom 2 (from β-barrel or cAMP)	Distance (Å)
Tyr371 OH	Glu324 OE2	3.2
Asn372 O	cAMP N6	3.4
Ser373 OG	Gln302 OE1	3.2
Phe374 N	Gln302 OE1	3.4
Phe374 N	Gln302 NE2	2.8
Val375 N	Gln302 OE1	3.1

Table 3. Hydrophobic Interactions Involving the C-Terminal Tail when cAMP Bounded

Residue 1 (from C Tail)	Residue 2 (from β-barrel or cAMP)	Distance (Å)
Ser361	Leu328	3.5
Ile363	Ile253	4.4
Leu364	Ile253	3.7
Leu364	Tyr321	3.6
Leu364	Phe353	3.8
Lys365	Leu328	3.6
Lys365	Met329	3.8
Ile368	Ile325	4.2
Ile368	Met329	4.1
Tyr371	Ile325	3.8
Tyr371	cAMP	3.5
Phe374	Val311	3.8
Phe374	Val313	4.6

from Leu357 to Ser376 at the end of the C-terminal tail. The last three residues, Leu377-Ser378-Val379, are disordered due to the lack of electron density in both 2Fo-Fc and Fo-Fc maps, as shown in Figure 1C. These last three residues also are not seen in the cAMP-bound structure (Su et al., 1995). In the absence of the B site cAMP, all of the interactions between cAMP, the C terminus, and β-barrel core of domain B are removed. Tyr371, a key residue for cAMP binding, is now far from the B site pocket due to the rotation of its aromatic ring by more than 110°; it does not make any close contact with other residues. All of the other C-terminal residues (Asn372–Val375) are also 9–14 Å from the cAMP binding pocket in the B site in the RIα cAMP-free structure. Phe374, which anchors the C helix to the β4-β5 loop in the cAMP-bound state, now has a new hydrophobic environment due to crystal packing. The aromatic ring of Phe374 plugs into the A site pocket from another symmetry-related molecule and sandwiches the guanine ring of the cGMP in the A site with Trp260 on the other side.

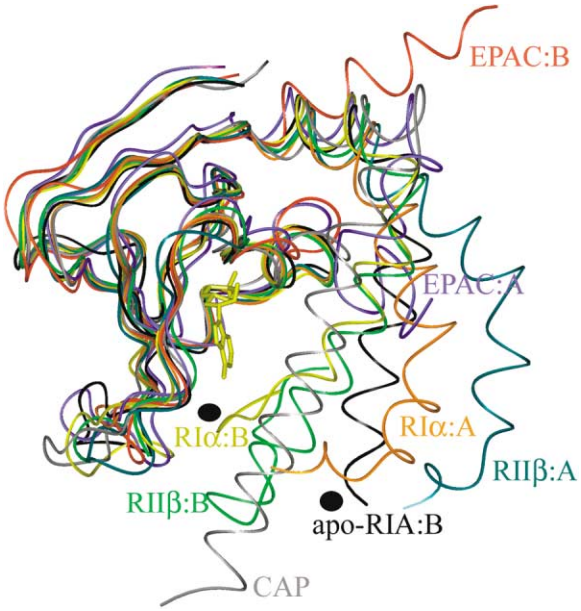

Figure 4. Superimposition of cAMP Binding Domains

cAMP-bound RIα, RIIβ, and CAP; cAMP-free EPAC and RIα are color coded, respectively. The apo-RIα:B corresponds to the cAMP-free domain B, the RIα:A and RIα:B to the cAMP-bound domains. The black circles are added to highlight the cAMP-bound and -free forms of RIα.

Cyclic Nucleotide Binding Sites

There are two cAMP binding domains (CBD), site A and site B in the RIα subunit of PKA. Site A is still occupied by cyclic GMP, while site B is ligand-free in this crystal structure as described above. The residual cGMP in site A derives from the cGMP-elution during purification. As shown as Figure 2A, domain A with cGMP bound shows no significant conformational change compared to the cAMP-bound form. The cyclic GMP is anchored within the center of the β-barrel by a similar network of contacts found in the cAMP-bound RIα structure. A comparison of a portion of the other seven cAMP binding domains for which structures are known shows that the general features of each cAMP binding domain, evidenced by each site's hydrogen-bonding pattern are highly conserved, even when occupied by cGMP in this case. Unlike the stable CBD core, the guanine ring of cGMP is obviously perturbed. When cGMP occupies the cAMP binding site, the phosphate and the ribose ring are buried in the same position as cAMP through several hydrogen bonds and electrostatic contacts. However, the cGMP guanine ring faces outside the pocket, and moves a little away from Ala210 to avoid a 2.4 Å close contact between the N2 atom of cGMP that is absent in cAMP and the C_β of Ala210. This position is always a Thr in cGMP-dependent protein kinase (PKG) and an Ala in PKA. Replacement of this Ala with Thr in the RIα subunit improved specificity for cGMP but did not weaken the affinity for cAMP (Shabb et al., 1991).

The cAMP binding domains contain a highly conserved signature motif, designated as the phosphate binding cassette (PBC) within the middle of the β-barrel (Diller et al., 2001). The PBC consists of β strand 6 followed by a short helix and loop and then β strand 7. The absence of the cyclic nucleotide in domain B of the RIα subunit leads to significant changes around the PBC that suggests increased dynamics or disorder. The PBC motif adopts a similar C_α trace overall compared to cAMP-bound form, although the electron density around the backbone of this segment is poorly traced or even partially discontinuous. In addition, most of the side chains of PBC residues are disordered when the cyclic nucleotide is absent in site B, suggesting that the PBC motif is more flexible. A plot of the B factors (Figure 2B) also confirms that this segment (residues 320–340) is highly dynamic. The side chain of Glu324 is still visible due to a hydrogen bond with its own backbone amide, although it adopts a different orientation relative to the cAMP bound structure. Arg333, a major residue that contributes to cAMP binding by interacting with the equatorial exocyclic oxygen of the cAMP phosphate, shows side chain disorder. A glycerol molecule occupies the position of the phosphate and ribose ring, but it makes only one hydrogen bond to the backbone amide of Ala326. The network of hydrogen bonds and hydrophobic interactions apparently cannot be sustained in the absence of the cyclic nucleotide, although the overall β-barrel remains intact. The empty PBC motif has a very similar conformation to its conformation when cAMP is bound. Upon binding into the PBC pocket, cAMP can stabilize both itself and the cAMP binding domain by nucleating an extensive network of contacts.

Superposition of the ligand-bound cAMP binding domains of CAP, PKA RIα and RIIβ with cAMP-free domains of EPAC and this cAMP-free PKA RIα B domain shows the variability of the C helix relative to these highly conserved cAMP binding sites (Figure 4). Although the structure of EPAC in the presence of cAMP is not known, this comparison suggests that the C-terminal tail adopts a common hinge mechanism for the cAMP binding and release (Diller et al., 2001: Rehmann et al., 2003). In the cAMP-bound structures of RIα and RIIβ of PKA, this tail region stabilizes cAMP binding to site B via the extensive network of contacts described above.

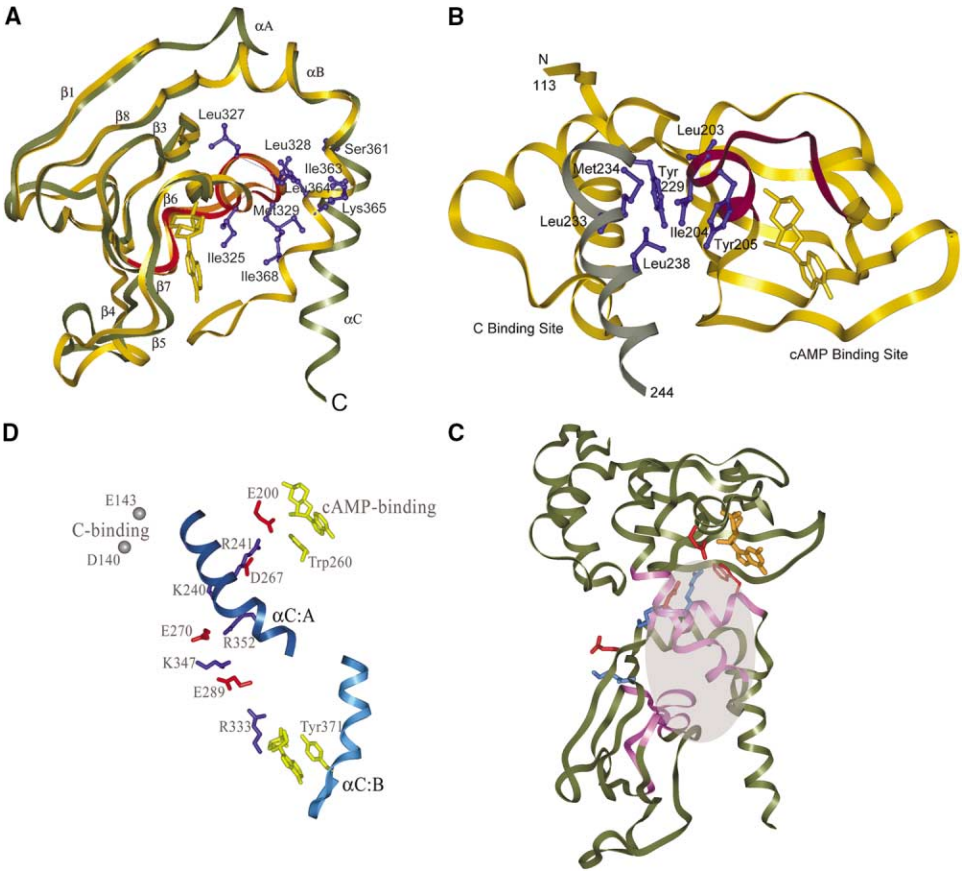

Figure 5. Interdomain Communication in RIα Subunit

(A) The hydrophobic pocket between the PBC motif and the C-terminal tail is highlighted. All of the hydrophobic side chains are shown in blue and labeled. The ribbons are shown in yellow in cAMP-bound RIα and in dark green in cAMP-free RIα.

(B) The hydrophobic core of site A. Those hydrophobic side chains are shown in blue and labeled. The C helix is shown in gray, and the other ribbons in yellow.

(C) Interdomain communication between site A and site B. The hydrophobic core is shadowed, and shown in purple. The electrostatic pathway, indicated by the arrow, shows (in red) the negatively charged residues, and (in blue) the positively charged residues.

(D) The specific electrostatic residues that link sites A and B. The side chains of the negatively charged residues are shown in red, and the positively charged residues in blue. The C helices in domain A and B are also shown.

Hydrophobic Pocket Network

In the cAMP-bound RIα structure, there is a hydrophobic pocket between the B site PBC motif and the hydrophobic side of the C helix at the carboxyl terminus, as shown as Figure 5A. The stable core is mostly composed of hydrophobic residues: Ile325, Leu327, Leu328, and Met329 from B site PBC on one side, and Ile363, Leu364, Ile368, and the side chains of Ser361 and Lys365 from the C helix on the other side. It appears that this hydrophobic core plays a role in communicating between the PBC motif in the β-barrel center and the carboxyl terminus by a ligand-dependent mechanism. A similar hydrophobic hinge between the cAMP binding domain and the C-terminal motif that may induce the rearrangement of neighboring residues was predicted previously based on the crystal structure of cAMP-free EPAC (Rehmann et al., 2003). When cAMP is removed from the B site pocket, the PBC motif appears to be highly dynamic, and all of the hydrophobic PBC residues except Leu328 are disordered based on the cAMP-free crystal structure. This may then leave the hydrophobic core exposed to solvent, eventually forcing a "hinge" movement of the C helix. The latter movement induces the C helix together with the rest of carboxyl terminus to move further away from the B site pocket. This "gate opening" is clearly observed when the cAMP-free structure is compared to the cAMP bound structure.

It is interesting to note that a similar hydrophobic pocket also exists in the A site, as shown in Figure 5B. The hydrophobic side chains of Leu233, Met234, and Leu238 from the C helix, and Leu203, Ile204, and Tyr205 from the PBC motif of domain A are packed against each other and provide the connection between the two subdomains (Anand et al., 2002).

Another network of hydrophobic interactions extends through β strand 3, the A helix of domain B, and the C helix of domain A to cAMP A site (Figure 5C). Many hydrophobic side chains converge to create this stable core. The core region seems to be centered on β strand 3 of domain B and the C helix of domain A, which consists of Phe290, Phe291, Ile292, Ile293, and Leu294 from β strand 3, and Phe247, Leu248, Val251 from the C helix

of the domain A as well as Ile253 and Leu254 from the loop that follows the C helix. In addition to those PBC residues mentioned above, Tyr321 and Phe322 are also involved by forming multiple hydrophobic interactions with the center of the core. The A helix of domain B that forming direct hydrophobic contacts to cAMP bound to the A site by stacking the aromatic ring of Trp260 up against the adenine ring of cAMP, also makes an extensive network of hydrophobic interactions with the core by the residues of Leu263, Val265, Ala266, Ala268, and Leu269. The network of hydrophobic interactions may be further enhanced by the complex pathway of electrostatic contacts from the cAMP B site to A site (Figure 5D). First, Arg333 that hydrogen bonds directly to cAMP bound to the B site makes a salt bridge interaction to Glu289. It is then followed by a charge relay pathway comprised of Lys347, Glu270, Lys240, Asp267, Arg241, and Glu200. Glu200 is part of the PBC in domain A and hydrogen bonds directly to the ribose OH of cAMP at A site. These two lines of communication may play critical roles in linking the PBC motif in the B site to the remote A site. In the cAMP-free structure, the C helix of domain A shows a small perturbation and somewhat higher B factors compared to the cAMP-bound form. Unfortunately, a cyclic GMP still occupies the A site in this crystal structure, which may prevent any significant conformational changes from occurring in the A site pocket and the C helix lid on domain A.

Discussion

To fully understand the dynamic process associated with ligand binding requires not only static high-resolution crystal structures which capture unique conformational states but also solution methods that reflect those changes in real time. The dynamic behavior of the cAMP binding domains of RIα in solution has been demonstrated by several methods. A combined method of site-directed labeling and time-resolved fluorescence anisotropy was used to characterize the dynamic features of the RIα subunit (Li et al., 2000). To specifically monitor changes associated with cAMP binding to site B, Ser373 on the C-terminal tail was replaced with Cys, and then modified with fluorescien. The removal of cAMP dramatically decreased the ϕ_{fast} values from 3.2 to 2.1 ns, and ϕ_{slow} range from 60–89 to 47–68 ns indicating that the backbone flexibility around the carboxyl terminus, specifically around the mutation site, significantly increases when cAMP is removed from site B. This is completely consistent with the structure we observed here. This enhanced mobility persisted when the C subunit was bound.

Another method for evaluating conformational changes in solution is hydrogen/deuterium (H/D) exchange, coupled with mass spectrometry. When the Δ(1-91) RIα subunit was probed in the presence and absence of cAMP, it was found that the overall changes in H/D exchange in the cAMP binding domains are relatively small when cAMP is removed, especially in the PBC region (Anand et al., 2002). This is also confirmed by molecular dynamics calculations, coupled with small angle X-ray scattering (D. Vigil and S.S.T., unpublished data). The major difference, in the absence of cAMP, is the increased dynamics of the PBC motifs at both A site (Anand et al., 2002) and B site and the carboxyl terminus, as measured by a significant increase in backbone amide exchange (Y. Hamuro et al., submitted).

Genetic evidence highlights the importance of the C-terminal tail. A yeast *bcy*1 C-terminal deletion mutant (*bcy*1-53) where only a portion of the C helix corresponding to the short tail of domain B was deleted was analyzed for stationary phase-specific defects (Cannon et al., 1990; Peck et al., 1997). These studies indicated that the *bcy*1-53 deletion mutant had lower cAMP-dependent kinase activity although the cAMP level in *bcy*1-53 extract was equivalent to the wild-type extract. These data showing that kinase activation is diminished indicates that the C-terminal region of *bcy*1p is essential for the modulation of *bcy*1p function during growth in the stationary phase. Our structure predicts that deletion of the C helix would disrupt the allosteric mechanism of activation.

Two different conformational states of this cAMP binding motif are now known based on the crystal structures of cAMP-free and cAMP-bound RIα subunits. In the absence of the B site cAMP, the PBC motif at domain B is highly dynamic and the carboxyl terminus is extended away from the binding pocket reflecting an opening of the "gate." When cAMP is bound, the PBC motif and cAMP constitute a highly conserved structural core maintained by an extensive network of contacts, with the C-terminal tail sealing the cAMP into B site by making interactions with both the PBC motif and ligand. Based on these two structures, a reasonable hypothesis can be posed. Allosteric activation of the type I holoenzyme is a concerted process that involves communication between four sites—(1) cAMP binding site B, (2) cAMP binding site A, (3) the peripheral C subunit binding site, and (4) the consensus peptide site in the linker region. The locations of the first three sites are highlighted in Figure 6. For the holoenzyme complex of PKA, cAMP binds first to site B, since the domain A of RIα subunit is masked or inactive when the catalytic subunit is bound. Our structure shows site B to be open, poised for cAMP to bind. Following the binding of cAMP, the PBC motif and the rest of domain B will be stabilized and all of the contributing side chains will be positioned, especially Glu324, and the hydrophobic residues Ile325, Leu328, and Met329. This "capping" will induce a hinge movement of the C helix at the carboxyl terminus to form a stable hydrophobic core. The latter movement will position the C-terminal tail so that it seals the cAMP into the B site pocket, which accounts for the higher affinity cAMP binding site and the lower off-rate. This conformational switch can also be sensed by the domain A since the N-terminal region of the C helix is linked to the A helix and both are in direct proximity to cAMP binding site A. We now provide a molecular explanation for the obligatory ordered binding of cAMP first to site B and then to site A and a mechanism for the allosteric communication between site B and site A.

The early work of Ogreid suggested that there was a mechanism for activation of RIα with cAMP binding first to domain A and then to domain B (Ogreid and Doskeland, 1981a, 1981b). This hypothesis was reinforced by

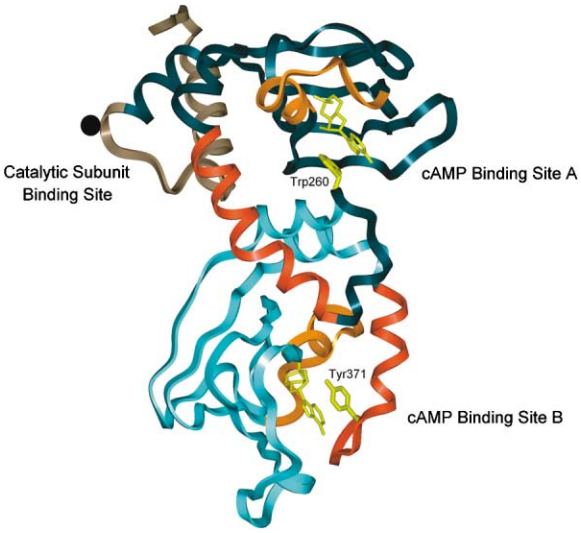

Figure 6. The Domain Organization and the Functional Sites of RIα Are Highlighted

Domain B is in light blue, domain A is dark blue, and the N-terminal segment preceding the domain is in tan. The C helices and PBC motifs in domain A and B are shown in red and orange, respectively.

mutants where the essential Arg in each cAMP binding domain was replaced with Lys thereby effectively reducing affinity for cAMP. The properties of these mutants were totally consistent with a "gatekeeper" model (Herberg et al., 1996). In neither case could activation be achieved until sufficient cAMP was present to bind to the mutated site. When site B was mutated, cAMP could not bind to site A in the holoenzyme even though it could bind readily to site A in the free R subunit. Likewise, when site A was mutated, activation was not achieved until there was sufficient cAMP to saturate the mutated A site. There are two explanations for having a nonfunctional site A in the holoenzyme. cAMP binding site A could be sterically blocked when site B is not occupied; alternatively, cAMP binding site A could be altered and nonfunctional when site B is unoccupied. Our structure does not discriminate between these two models. It does, however, describe two long distant lines of communication, one hydrophobic and one electrostatic, between site A and site B. These sites provide a mechanism for sensing whether cAMP is bound to the other site.

These cAMP binding domains in general, based on crystal structures of RIα, RIIβ, CAP, EPAC, and the cAMP-gated channel, share a highly conserved structural core and a similar hydrogen-bonding network, which implies they may adopt a similar mechanism for cAMP binding and release. The comparison of seven cAMP binding domains (Figure 4) indicates the variability of the C-helical region relative to the CBD core. The structure described here provides a mechanism for regulation of the position of the C helix of domain A by domain B which provides a concerted pathway to site A through the hydrophobic core and an electrostatic pathway. Obviously, the structure of a cyclic nucleotide-free domain A as well as a holoenzyme structure are still needed to fully understand the allosteric communication between these two domains. Clearly the C terminus of the cAMP binding domain is the most variable part of this conserved motif and will be regulated in unique ways in each protein. Here we see clearly how domain B in RIα can regulate or communicate with the cAMP binding site in domain A.

Experimental Procedures

Preparation of cAMP-free Protein

The recombinant Δ(1-91) RIα were expressed in *Escherichia coli* 222 cells. The proteins were purified as described previously (Saraswat et al., 1988) using cAMP-agarose resin. The R subunits of PKA are typically purified in the presence of cAMP. It is not possible to remove the cAMP by dialysis; mild denaturants are typically used. To avoid urea treatment, Δ(1-91) RIα was purified by cAMP-affinity resin and then eluted with 25 mM cGMP (J.M. Jones, personal communication). Unlike cAMP, this cGMP can be readily removed by dialysis. The protein elutes were dialyzed against 50 mM MES buffer at pH 7.5 with 200 mM NaCl, 2 mM EDTA, 2 mM EGTA, 10 mM DTT with buffer changing once at 4°C overnight, and concentrated to 10 mg/ml. The protein concentration was measured by a Bradford assay using bovine serum albumin as standard.

Crystallization and Data Collection

The cAMP-free Δ(1-91) RIα was crystallized against the reservoir solution (1.0 M NH_2SO_4, 12.5% glycerol, 10 mM DTT, 0.1 M Tris-HCl buffer at pH 7.5) at 22.5°C using the hanging drop vapor-diffusion method. Crystals were harvested within 3–4 weeks. The crystallization condition except the pH value is similar to that used for the cAMP-bound Δ(1-91) RIα (Su et al., 1995). Crystals were flash frozen in the liquid nitrogen stream mounted by nylon loops, after dipping them in cryo-protectant solution (1.1 M NH_2SO_4, 25% glycerol, 10 mM DTT, 0.1 M Tris-HCl buffer, pH 7.5).

Diffraction data was collected up to 2.7 Å resolution using one single crystal, after a wild screen of more than 80 crystals, at the Advanced Light Source (ALS). The crystal belongs to hexagonal space group $P6_5$ with the unit cell dimensions of a = b = 90.3 Å, and c = 177.6 Å (Table 1). There are two molecules in an asymmetric unit. Data was processed and scaled using HKL2000 (Otwinowski and Minor, 1997).

Structure Refinement

Phasing of cAMP-free RIα was generated by applying the difference Fourier method based on the crystal structure of cAMP-bound RIα, in which two cAMP were omitted. The structure refinement was performed using the CNS program (Brunger et al., 1998) on a Silicon Graphics O2 workstation. Ten percent of the data were randomly selected as the test data set used for cross validation. Rigid body refinement was carried out first. The structure was then refined for both simulated annealing from 2500°C and individual B factor for a number of rounds using CNS protocols. During the refinement, the (2Fo-Fc) and (Fo-Fc) electron density maps were regularly calculated and used for manually rebuilding the model. Model building was performed using the graphics software TURBO-FRODO (Roussel and Cambillau, 1991). The simulated annealing "omit" maps were calculated as well when necessary.

Acknowledgments

We thank Jie Yang and Ganesh Anand for thoughtful discussions. We thank the staff at ALS for help with data collection. Thanks to Elzbieta Radzio-Andzelm and Yuliang Ma for help with figures preparation; and to Debin Huang and Xueyong Zhu for help of HKL2000. This work was supported by a grant from the National Institutes of Health (GM 34921) to S.S.T.

Received: January 8, 2004
Revised: March 11, 2004
Accepted: March 15, 2004
Published: June 8, 2004

References

Anand, G.S., Hughes, C.A., Jones, J.M., Taylor, S.S., and Komives, E.A. (2002). Amide H/2H exchange reveals communication between the cAMP and catalytic subunit-binding sites in the R(I)alpha subunit of protein kinase A. J. Mol. Biol. *323*, 377–386.

Banky, P., Roy, M., Newlon, M.G., Morikis, D., Haste, N.M., Taylor, S.S., and Jennings, P.A. (2003). Related protein-protein interaction modules present drastically different surface topographies despite a conserved helical platform. J. Mol. Biol. *330*, 1117–1129.

Brunger, A.T., Adams, P.D., and Clore, G.M. (1998). Crystallography & NMR system: a new software suite for macromolecular structure determination. Acta Crystallogr. D *54*, 905–921.

Bubis, J., Saraswat, L.D., and Taylor, S.S. (1988). Tyrosine-371 contributes to the positive cooperativity between the two cAMP binding sites in the regulatory subunit of cAMP-dependent protein kinase I. Biochemistry *27*, 1570–1576.

Cannon, J.F., Gitan, R., and Tatchell, K. (1990). Yeast cAMP-dependent protein kinase regulatory subunit mutations display a variety of phenotypes. J. Biol. Chem. *265*, 11897–11904.

de Rooij, J., Zwartkruis, F.J., Verheijen, M.H., Cool, R.H., Nijman, S.M., Wittinghofer, A., and Bos, J.L. (1998). Epac is a Rap1 guanine-nucleotide-exchange factor directly activated by cyclic AMP. Nature *396*, 474–477.

Diller, T.C., Madhusudan, Xuong, N., and Taylor, S.S. (2001). Molecular basis for regulatory subunit diversity in cAMP-dependent protein kinase: crystal structure of the type II beta regulatory subunit. Structure *9*, 73–82.

Døskeland, S.O., Øgreid, D., Ekanger, R., Sturm, P.A., Miller, J.P., and Suva, R.H. (1983). Mapping of the two intrachain cyclic nucleotide binding sites of adenosine cyclic 3′,5′-phosphate dependent protein kinase I. Biochemistry, *22*, 1094–1101.

Herberg, F.W., Taylor, S.S., and Dostmann, W.R. (1996). Active site mutations define the pathway for the cooperative activation of cAMP-dependent protein kinase. Biochemistry *35*, 2934–2942.

Huang, L.J., and Taylor, S.S. (1998). Dissecting cAMP binding domain A in the RIalpha subunit of cAMP-dependent protein kinase. Distinct subsites for recognition of cAMP and the catalytic subunit. J. Biol. Chem. *273*, 26739–26746.

Kawasaki, H., Springett, G.M., Mochizuki, N., Toki, S., Nakaya, M., Matsuda, M., Housman, D.E., and Graybiel, A.M. (1992). A family of cAMP-binding proteins that directly activate Rap1. Science *282*, 2275–2279.

Li, F., Gangal, M., Jones, J.M., Deich, J., Lovett, K.E., Taylor, S.S., and Johnson, D.A. (2000). Consequences of cAMP and catalytic-subunit binding on the flexibility of the A-kinase regulatory subunit. Biochemistry *39*, 15626–15632.

Ludwig, J., Margalit, T., Eismann, E., Lancet, D., and Kaupp, U.B. (1990). Primary structure of cAMP-gated channel from bovine olfactory epithelium. FEBS Lett. *270*, 24–29.

Mitra, S., Zubay, G., and Landy, A. (1975). Evidence for the preferential binding of the catabolite gene activator protein (CAP) to DNA containing the *lac* promoter. Biochem. Biophys. Res. Commun. *67*, 857–863.

Ogreid, D., and Doskeland, S.O. (1981a). The kinetics of association of cyclic AMP to the two types of binding sites associated with protein kinase II from bovine myocardium. FEBS Lett. *129*, 287–292.

Ogreid, D., and Doskeland, S.O. (1981b). The kinetics of the interaction between cyclic AMP and the regulatory moiety of protein kinase II. Evidence for interaction between the binding sites for cyclic AMP. FEBS Lett. *129*, 282–286.

Otwinowski, Z., and Minor, W. (1997). Processing of X-ray diffraction data collected in oscillation mode. In Methods in Enzymology, Volume 276, J.C.W. Carter and R.M. Sweet, eds. (New York: Academic Press), pp. 307–326.

Peck, V.M., Fuge, E.K., Padilla, P.A., Gomez, M.A., and Werner-Washburne, M. (1997). Yeast bcy1 mutants with stationary phase-specific defects. Curr. Genet. *32*, 83–92.

Rannels, S.R., and Corbin, J.D. (1981). Studies on the function of the two intrachain cAMP binding sites of protein kinase. J. Biol. Chem. *256*, 7871–7876.

Rehmann, H., Prakash, B., Wolf, E., Rueppel, A., De Rooij, J., Bos, J.L., and Wittinghofer, A. (2003). Structure and regulation of the cAMP-binding domains of Epac2. Nat. Struct. Biol. *10*, 26–32.

Ringheim, G.E., Saraswat, L.D., Bubis, J., and Taylor, S.S. (1988). Deletion of cAMP-binding site B in the regulatory subunit of cAMP-dependent protein kinase alters the photoaffinity labeling of site A. J. Biol. Chem. *263*, 18247–18252.

Roussel, A., and Cambillau, C. (1991). Turbo-Frodo, Silicon Graphics Partner Geometry Dictionary (Mountain View, CA: Silicon Graphics Inc.).

Rubin, C.S. (1994). A kinase anchor proteins and the intermolecular targeting of signals carried by cyclic AMP. Biochim. Biophys. Acta *1124*, 467–479.

Saraswat, L.D., Filutowics, M., and Taylor, S.S. (1988). Expression and mutagenesis of the regulatory subunit of cAMP-dependent protein kinase in Escherichia coli. Methods Enzymol. *159*, 325–336.

Scott, J.D. (1991). Cyclic nucleotide-dependent protein kinases. Pharmacol. Ther. *50*, 123–145.

Shabb, J.B., and Corbin, J.D. (1992). Cyclic nucleotide-binding domains in proteins having diverse functions. J. Biol. Chem. *267*, 5723–5726.

Shabb, J.B., Buzzeo, B.D., Ng, L., and Corbin, J.D. (1991). Mutating protein kinase cAMP-binding sites into cGMP-binding sites: mechanism of cGMP selectivity. J. Biol. Chem. *266*, 24320–24326.

Su, Y., Dostmann, W.R.G., Herberg, F.W., Durick, K., Xuong, N., Eyck, L.T., Taylor, S.S., and Varughese, K.L. (1995). Regulatory subunit of protein kinase A: structure of deletion mutant with cAMP binding domains. Science *269*, 807–813.

Taylor, S.S., Buechler, J.A., and Yonemoto, W. (1990). cAMP-dependent protein kinase: framework for a diverse family of regulatory enzymes. Annu. Rev. Biochem. *59*, 971–1005.

Walsh, D.A., Perkins, J.P., and Krebs, E.G. (1968). An adenosine 3′,5′-monophosphate-dependant protein kinase from rabbit skeletal muscle. J. Biol. Chem. *243*, 3763–3765.

Weber, I.T., and Steitz, T.A. (1987). Structure of a complex of catabolite gene activator protein and cyclic AMP refined at 2.5 A resolution. J. Mol. Biol. *198*, 311–326.

Wu, J., Johns, J.M., Xuong, N., Eyck, L.T., and Taylor, S.S. (2004) Crystal structures of RIα subunit of cyclic adenosine 5′-monophosphate (cAMP)-dependent protein kinase complexed with (*R*p)-adenosine 3′,5′-cyclic monophosphothioate and (*S*p)-adenosine 3′,5′-cyclic monophosphothioate, the phosphothioate analogues of cAMP. Biochemistry, in press.

Zagotta, W.N., Olivier, N.B., Black, K.D., Young, E.C., Olson, R., and Gouaux, E. (2003). Structural basis for modulation and agonist specificity of HCN pacemaker channels. Nature *425*, 200–205.

Accession Numbers

The coordinate and structure factor are deposited with the Protein Data Bank (PDB accession code 1RL3).